



EFFECTIVE POLYMER DECORATION ON NICKEL-IMINE COMPLEX TO ENHANCE CATALYTIC HYDROGEN EVOLUTION

^{1,*}Dilek KILINÇ , ²Ömer ŞAHİN

¹Harran University, Pharmacy Faculty, Pharmaceutical Chemistry Department, Şanlıurfa, TÜRKİYE

²Istanbul Technical University, Chemical and Metallurgical Engineering Faculty, Chemical Engineering Department, Istanbul, TÜRKİYE

¹ dkilinc@harran.edu.tr, ²sahinomer2002@yahoo.com

Highlights

- Preparation of polymer decorated Ni@EC, Ni@EC-250, Ni@ECM catalysts.
- Effectively enhanced catalytic NaBH₄ hydrolysis activity by polymer decoration.
- Excellent catalytic activity of Ni@EC-250 with 28689 mL H₂/g_{cat}.min HGR at 50 °C.
- High stability of catalyst in 5th recycles with 100 % conversion.
- Obtaining low activation energy of 39.255 kJ·mol⁻¹



EFFECTIVE POLYMER DECORATION ON NICKEL-IMINE COMPLEX TO ENHANCE CATALYTIC HYDROGEN EVOLUTION

^{1,*}Dilek KILINÇ , ²Ömer ŞAHİN

¹Harran University, Pharmacy Faculty, Pharmaceutical Chemistry Department, Şanlıurfa, TÜRKİYE

²Istanbul Technical University, Chemical and Metallurgical Engineering Faculty, Chemical Engineering Department, Istanbul, TÜRKİYE

¹dkilinc@harran.edu.tr, ²sahinomer2002@yahoo.com

(Received: 27.10.2023; Accepted in Revised Form: 18.12.2023)

ABSTRACT: Since fossil fuels are rapidly depleting, finding alternative energy sources is becoming increasingly important. Among these alternatives, hydrogen (H_2) is the most viable option. In hydrogen evolution systems, supported metal catalysts enhance the catalytic activity in the hydrolysis reaction by increasing the surface area. Therefore, this research focuses on preparing three different polymer-decorated Nickel-Imine complex catalysts (Ni@EC, Ni@EC-250, Ni@ECM) to improve their efficiency. To achieve the catalysts, a Nickel-Imine complex [1] was supported on three different polymers (EC, EC-250, and ECM). The catalysts (Ni@EC, Ni@EC-250, Ni@ECM) were then utilized to generate hydrogen from $NaBH_4$ hydrolysis. The hydrogen evolution rates for Ni@EC, Ni@EC-250, and Ni@ECM catalysts were found as 6879; 15576; 8830 and 15459; 28689; 23417 $mL\ H_2\ gcat^{-1}.min^{-1}$, respectively at 30 °C and 50 °C. Results indicate that the Ni@EC-250 catalyst exhibited the best activity. Consequently, the subsequent steps of the catalytic hydrolysis reaction were studied using Ni@EC-250. The activation energy of the Ni@EC-250 catalyst was estimated at 39.255 $kJ.mol^{-1}$. The reusability tests demonstrate that Ni@EC-250 remains active in sodium borohydride hydrolysis even after five runs. Technical abbreviations are defined upon first use. This study elucidates the reaction mechanism and kinetic data of catalytic sodium borohydride hydrolysis at various temperatures.

Keywords: Catalyst, Hydrogen evolution, $NaBH_4$, Ni-Imine, Polymer

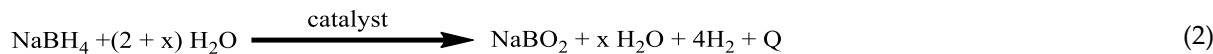
1. INTRODUCTION

Hydrogen evolution is a prominent renewable energy concern [2,3]. Hydrogen represents an environmentally friendly energy source and stands out as a favorable substitute for fossil fuels due to its non-toxic emissions, long-term viability, and energy security benefits [4]. As a safe and efficient source of clean energy carriers [5,6], chemical hydrides are advantageous hydrogen storage materials due to their high hydrogen densities [7,8]. Among the different chemical hydrides, sodium borohydride stands out as the preferred material due to its high H_2 capacity, stability, recyclability, non-flammability, and non-toxic chemistry [9, 10]. H_2 is produced from sodium borohydride through hydrolysis or thermolysis [11, 12]. However, since thermolysis reactions are not an economically feasible process and cannot be practically used, hydrolysis is the preferred reaction. Eq. 1 provides the general hydrolysis reaction of sodium borohydride.

*Corresponding Author: Dilek KILINÇ, dkilinc@harran.edu.tr



In the presence of water, the reaction is expressed as shown in Eq. 2.



In this case, x is referred to as the "hydration factor".

In hydrolysis, slow and controllable reactions with higher rates of H_2 evolution are obtained in objective systems using metal catalysts [13]. Numerous studies concerning the catalytic hydrolysis of sodium borohydride have been conducted by scientists for decades. Metal salts, alloys [14, 15], acids [16], or support materials [17] have been studied for this purpose. Due to the cost of noble metal catalysts, the usage of comparatively inexpensive non-noble metal catalysts is desired. Generally, the catalytic performance diminishes after each cycle in the hydrogen evolution reaction [18-20]. To counter this issue, incorporating a metal catalyst into a support material enhances the catalytic performance by expanding the catalyst surface area [21-23]. The chief issue remains to extract the metal catalyst from the reaction medium [24, 25], which can be effectively and practically addressed by using a supported catalyst [26, 27]. In the literature, various catalysts that support hydrolysis of sodium borohydride have been documented, including resin bead-supported Ru [26], poly-p-xylene supported Co [28], polymer-modified Co [29], Cu-ZrO₂ films [27], magnetically supported catalyst [24], Ni-Al₂O₃ [30, 31].

Polymers are widely used as support materials due to their high surface area, thermal stability, mechanical strength, and easy modification [32]. Furthermore, polymer-supported catalysts offer more environmentally friendly methods for various synthesis reactions than traditional methods. They have also enabled catalyst recycling [32, 33]. The polymer-supported catalytic system comprises robust polymer support and physical interactions. In recent years, imines and their compounds have received extensive research attention for their outstanding optical, thermal, electronic, and mechanical properties [34]. Furthermore, due to their straightforward synthesis and high electrical conductivity, imines and their metal complexes demonstrate remarkable photovoltaic effects [35].

Imines containing azomethine (-C=N-) bonds [36] exhibit an impressive ability to chelate with transition metals, lanthanide, or actinide ions forming imine complexes [35, 36]. Due to its versatile coordination compounds, with flexible and stereo-electronic structures, imine complexes have emerged with several applications such as plastic, aircraft, agriculture, cancer chemotherapy, drug production, antifungal, anti-inflammatory, antibacterial, and antiviral reactions, space, and electronics industries [37]. However, only a few studies exist about Imine complexes used in catalytic hydrogen evolution systems [38, 39].

In this paper, we examine the impact of three varied polymer-decorated Nickel-Imine catalysts (Ni@EC, Ni@ECM, and Ni@EC-250). Our study had two goals: (i) to enhance the catalytic activity of the Nickel-Imine complex by utilizing distinct polymer decoration in sodium borohydride hydrolysis reaction, which would lead to better interaction between the catalysts and sodium borohydride, and (ii) to determine the most efficient polymer-decorated catalyst for this reaction. The hydrogen evolution rates for Ni@EC, Ni@EC-250, and Ni@ECM catalysts were calculated from the experimental results. At 30 °C and 50 °C, they were found as 6879; 15576; 8830 and 15459; 28689; 23417 mL H₂ gcat⁻¹.min⁻¹, respectively. In comparison, the pure Nickel-Imine complex exhibited only 2240 and 10983 mL H₂ gcat⁻¹.min⁻¹ at the same temperatures [1]. Therefore, it can be concluded that the polymer decoration significantly increased the hydrogen evolution rate. Between the three catalysts, Ni@EC-250 demonstrated superior activity compared to the others under identical conditions. Henceforth, the other stages of catalytic hydrolysis reaction were examined using Ni@EC-250. The activation energy of the Ni@EC-250 catalyst was estimated at 39.255 kJ.mol⁻¹. The recycle tests revealed that Ni@EC-250 remains active in sodium borohydride hydrolysis even after five cycles. This report presents the reaction mechanism and kinetic data of catalytic hydrolysis of sodium borohydride at varying temperatures.

2. MATERIAL AND METHODS

2.1. Materials

All chemicals and solvents used were supplied by Merck, without undergoing any purification.

All samples were subjected to XPS studies to analyze the chemical states of the polymer-decorated nickel complex catalysts, using a Flex Specs electron spectrometer.

The Perkin-Elmer model FT-IR spectrometer was used to record Fourier Transform Infrared (FT-IR) spectra of the samples in the 4000-400 cm⁻¹ range.

The Ni@EC, Ni@EC-250, and Ni@ECM samples underwent measurement of their surface areas using the Brunauer-Emmett-Teller (BET) theory by BET surface area measurement.

To identify their crystal structures, X-ray diffraction (XRD) patterns were measured for Ni@EC, Ni@EC-250, and Ni@ECM with Rigaku Cu K α ($\lambda = 154.059$ pm) radiation at a scanning rate of 5 °C min⁻¹ within the range of 2θ=0-80°.

The electronic behavior of the catalysts Ni@EC, Ni@EC-250, and Ni@ECM was investigated through the use of a Perkin-Elmer model UV-Vis spectrometer, ranging between 250 and 800 nm.

To examine the microstructure and morphology of these catalysts, a JEOL JSM 5800 model scanning electron microscope (SEM) was utilized.

2.2. Synthesis of the Catalyst

Step1: Synthesis of the Imine ligand

The ligand was synthesized by adding 1 mmol of 3,5-ditertbutylsalisylaldehyde (30 ml of ethanol) to 5-Amino-2,4-dichlorophenole (20 ml of ethanol) and refluxing the mixture at 80 °C for 5-6 h, as described in our earlier study [1].

Step 2: Synthesis of the Nickel-Imine complex

The Nickel-Imine complex was synthesized under mild conditions using 40 mM of 5-Amino-2,4-dichlorophenol-3,5-di-tertbutyl salicylaldimine ligand and 20 mM of NiCl₂.6H₂O in 20 mL of ethanol, following the procedures outlined in our previous study [1].

Step 3: Preparation of the polymer-decorated Nickel-Imine complex catalysts

Ni@EC, Ni@EC-250, and Ni@ECM catalysts were prepared using a precipitation technique with Nickel-Imine complex [1] and EC, ECM, and EC-250 polymers. Technical abbreviations are explained on first use. To do this, 100 mg of the polymer was added to an ethanolic solution of Nickel-Imine complex at different concentrations (1 %, 5%, 10 %, 15 %, and 20 %) and stirred for approximately 72 hours at room temperature. The obtained catalysts, Ni@EC, Ni@ECM, and Ni@EC-250, were filtered, washed with ethyl alcohol, and finally dried at 70°C. The diagrammatic representation of catalysts comprising nickel complexes coated with polymers (Ni@EC, Ni@ECM, and Ni@EC-250) is depicted in Figure 1.

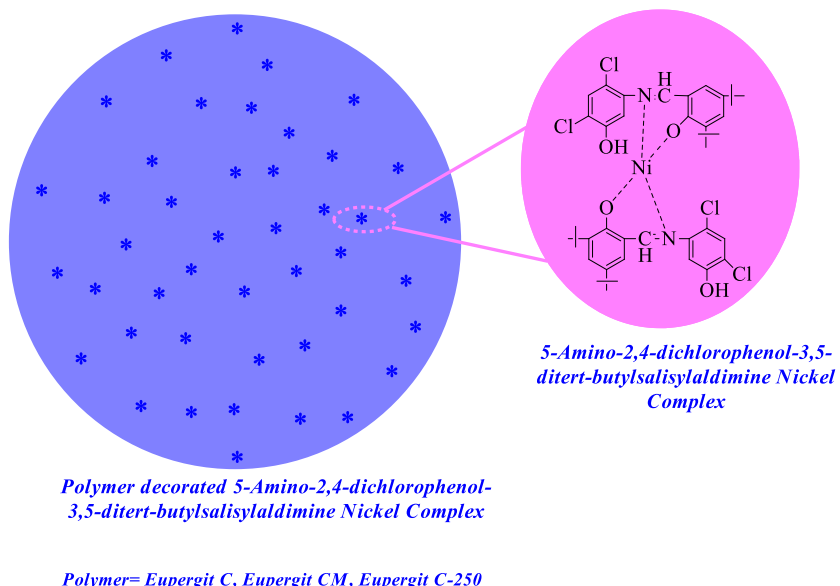


Figure 1. Schematic illustration of polymer decorated Nickel-Imine complex (Ni@EC, Ni@EC-250, Ni@ECM)

2.3. Catalytic Hydrogen Evolution Performance

Various experiments were conducted on hydrogen evolution using Nickel-Imine catalysis with different polymers. The experiments took place at 30°C in an aqueous solution containing 2 % NaBH₄, 10 % NaOH, and 15 mg catalyst. The concentration of Nickel-Imine complex varied for each experiment. The hydrogen evolution system was implemented through the water-gas displacement method. For various Nickel-Imine catalysts decorated with different polymers (Ni@EC, Ni@EC-250, and Ni@ECM), comparative experiments were conducted to determine the hydrogen evolution rates. The most effective catalyst was selected and further tested.

3. RESULTS AND DISCUSSION

3.1. Catalytic Studies

3.1.1. Hydrogen evolution activities

Several experiments were conducted to identify the most effective polymer-decorated Nickel-Imine with the highest catalytic activity for the hydrolysis of NaBH₄ to release hydrogen. As a result, the catalytic hydrolysis of NaBH₄ was examined under the same reaction conditions using 5 % Ni complex, 15 mg catalyst (Ni@EC, Ni@EC-250, and Ni@ECM), 10 % NaOH, and 2 % NaBH₄ at 30 °C. In this reaction medium, hydrogen evolution rates of 6,879 mL H₂ gcat⁻¹.min⁻¹, 15,576 mL H₂ gcat⁻¹.min⁻¹, and 8,830 mL H₂ gcat⁻¹.min⁻¹ were calculated, as shown graphically in Figure 2. It is evident that, under the same reaction

conditions, Ni@EC-250 exhibited the highest catalytic activity, compared to Ni@EC and Ni@ECM. The catalytic activity increased in the order of Ni@EC-250 > Ni@ECM > Ni@EC, with the inclusion of polymer into the Nickel-Imine complex structure. Therefore, other catalytic hydrolysis experiments were conducted using the Ni@EC-250.

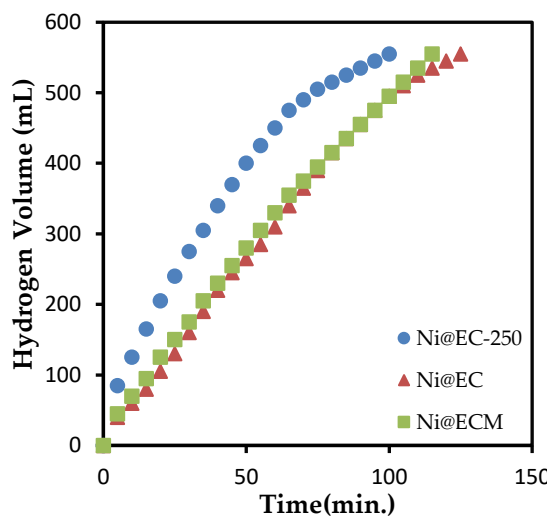


Figure 2. Plot of hydrogen volume versus time with different Ni catalysts

To determine the extent of Ni@EC-250 catalyzed hydrolysis reaction, the first step was to establish the quantities of their Ni complexes. To achieve this, the catalytic activity of Ni@EC-250 was investigated with varying concentrations of Ni complexes (1 %, 5 %, 10 %, 15 %, and 20 %) loaded onto 15 mg polymer-decorated nickel complex catalysts, as shown in Figure 3. To assess the impact of different Ni complex concentrations (1 %, 5 %, 10 %, 15 %, 20 %), the rates of hydrogen evolution were determined as 28,907; 15,576; 9,905; 7,708; 5,401 mL H₂ gcat⁻¹.min⁻¹, respectively. While 1 % Ni complex exhibited the highest catalytic activity, the hydrolysis reaction was incomplete resulting in a lower H₂ volume (only 370 mL H₂) than the calculated value (560 mL). According to the results, the use of a 5 % nickel complex produced faster hydrogen evolution rates than excessive concentrations for Ni@EC-250 catalyst. However, using over 5% nickel-imine complex caused a decrease in hydrogen evolution rates and catalytic activities. This reduction is due to the saturation of the catalyst surface with 5 % Ni complex, which occurs as the concentration of nickel complex increases.

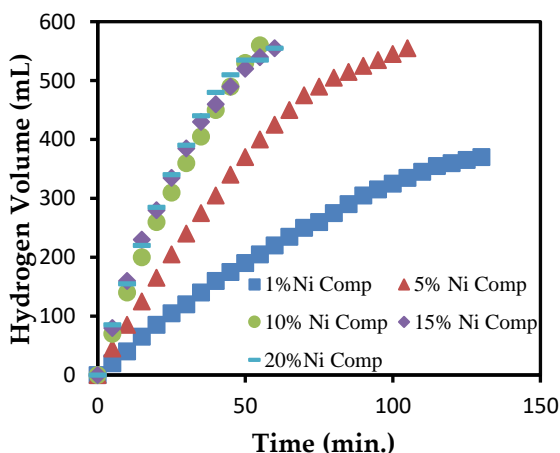


Figure 3. Plot of hydrogen volume versus time with various nickel complex concentrations in Ni@EC-250 catalyst

The impact of sodium hydroxide concentration on Ni@EC-250 catalyzed sodium borohydride hydrolysis is illustrated in Figure 4. The reaction mixture was prepared using 5% Nickel-Imine complex and 15 mg Ni@EC-250 in a 2 % sodium borohydride solution at 30°C. The rates of hydrogen evolution were determined through the addition of 0 %, 3 %, 5 %, 7 % and 10 % NaOH concentrations, resulting in respective rates of 7514; 7403, 9204; 14161 and 15576 mL H₂ gcat⁻¹.min⁻¹. According to the results, hydrogen evolution rates catalyzed by Ni@EC-250 increased as the sodium hydroxide concentration increased from 0 % to 10 %. At higher NaOH concentrations, the interaction of hydroxyl ions with free water molecules made the required water for the hydrolysis reaction easily accessible, increasing hydrogen evolution rates. In addition, the increase in sodium hydroxide concentrations led to shorter completion times of the hydrolysis reaction.

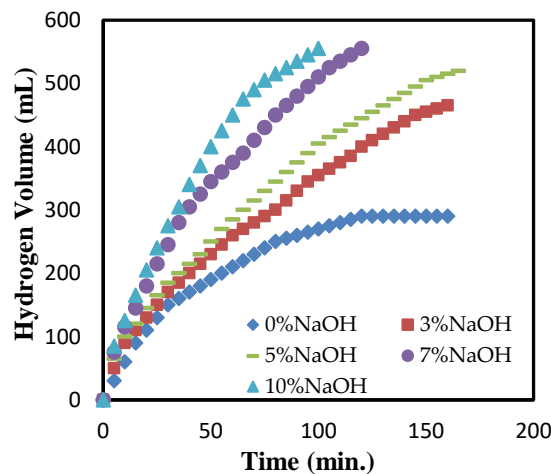


Figure 4. Plot of hydrogen volume versus time with various NaOH concentrations with Ni@EC-250 catalyst

In the sodium borohydride hydrolysis process, the influence of the Ni@EC-250 catalyst amount was presented in Figure 5. The reaction mixture resulted from a 5 % Nickel-Imine complex in a 2 % sodium borohydride solution at 30 °C. To apply 5mg, 15mg, 25mg, and 50mg of the catalyst, hydrogen evolution rates were determined as 10622; 15576; 26095 and 27284 mL H₂ gcat⁻¹.min⁻¹, respectively. According to the outcomes, the increment in the catalyst amount led to a reduction in reaction times. Ni@EC-250 catalyzed hydrogen evolution rates increased as the amount of catalyst increased from 5 mg to 50 mg. With more catalysts, the reactants were exposed to a larger reaction area, and the residence time in the reactor was reduced, accelerating the hydrolysis process.

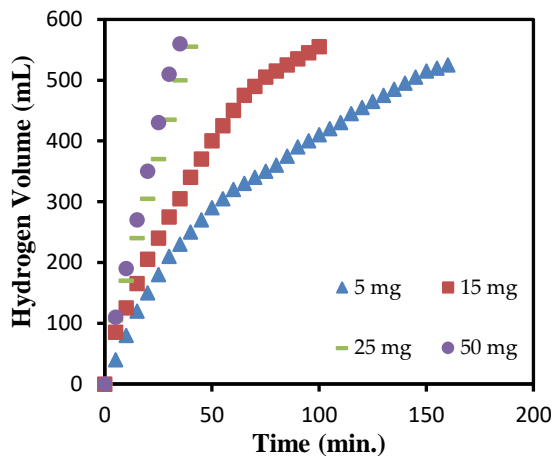


Figure 5. Plot of hydrogen volume versus time with various catalyst amounts with Ni@EC-250 catalyst

In Figure 6, the plot displays the relationship between hydrogen volume and time for a range of NaBH₄ concentrations. The reaction medium consisted of 5 % Nickel-Imine complex and 15 mg Ni@EC-250 catalyst in a 10 % sodium hydroxide solution at a temperature of 30°C. The hydrogen evolution rates catalyzed by Ni@EC-250 were calculated as 15576; 23089; 25415 and 26571 mL H₂ gcat⁻¹.min⁻¹ correspondingly, using 2 %, 5 %, 7 %, and 10 % sodium borohydride. An increase in gas volume was observed by increasing NaBH₄ concentration in the hydrolysis solution. The hydrogen evolution rates gradually increased with the increasing Ni@EC-250 catalyst and NaBH₄ concentration from 2 % to 10 %, as expected.

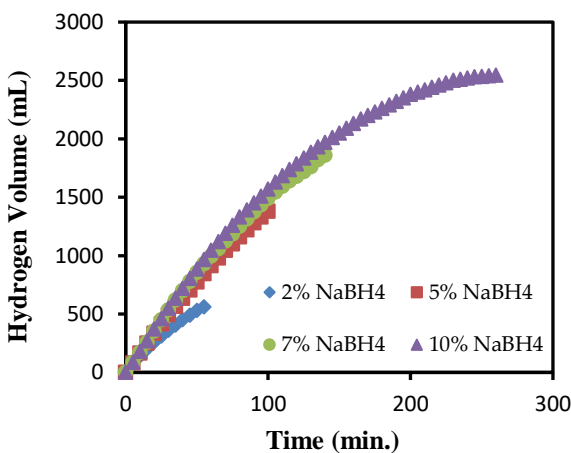


Figure 6. Plot of hydrogen volume versus time with various NaBH₄ concentrations with Ni@EC-250 catalyst

For the optimization of temperature effects, four different temperatures (20–50 °C) were studied. The reaction medium occurred from 5% Nickel-Imine complex, 15 mg Ni@EC-250 catalyst in 10 % sodium hydroxide-2 % NaBH₄ solution. Figure 7a displays the plot of hydrogen volume versus time with various temperatures with Ni@EC-250, catalyst in the range 20–50 °C. According to the experimental results, Ni@EC-250 catalyzed hydrogen evolution rates were calculated as 9329; 15576; 24740 and 28689 mL H₂ gcat⁻¹.min⁻¹ respectively. The reaction temperature increases positively affected the hydrogen evolution rates in this system. Four different temperatures (20–50 °C) were studied to optimize the temperature effects. The reaction medium consisted of 5 % nickel-imine complex, 15 mg Ni@EC-250 catalyst in 10 % sodium hydroxide-2 % NaBH₄ solution. Figure 7a shows the plot of hydrogen volume versus time with

different temperatures with Ni@EC-250, catalyst in the range 20-50 °C. According to the experimental results, the Ni@EC-250 catalyzed hydrogen evolution rates were calculated as 9329; 15576; 24740 and 28689 mL H₂ g_{cat}⁻¹.min⁻¹, respectively. Increasing the reaction temperature had a positive effect on the hydrogen evolution rates in this system.

3.1.2. Kinetic studies

The kinetic calculations for the hydrolysis of sodium borohydride, catalyzed by Ni@EC-250, can be determined using the equation for an nth-order reaction as seen in Eq. 3-6.

$$-r_{\text{NaBH}_4} = -\frac{dC_{\text{NaBH}_4}}{dt} = k \cdot C_{\text{NaBH}_4}^n \quad (3)$$

Separating and integrating, we get

$$-\int_{C_{\text{NaBH40}}}^{C_{\text{NaBH4}}} \frac{dC_{\text{NaBH4}}}{C_{\text{NaBH4}}^n} = k \int_0^t dt \quad (4)$$

$$\frac{1}{(n-1)} \left(\frac{1}{C_{\text{NaBH4}}} - \frac{1}{C_{\text{NaBH40}}} \right) = kt \quad (5)$$

$$\frac{1}{C_{\text{NaBH4}}^{n-1}} = (n-1)k \cdot t + \frac{1}{C_{\text{NaBH40}}^n} \quad (6)$$

According to Eq. 6, the hydrolysis reaction catalyzed by Ni@EC-250 had a reaction order (n) value of 0.2. The rate constants were determined from the linear portion of H₂ generation versus time between 20-50 °C, as shown in Figure 7b. The activation energy for Ni@EC-250 in the NaBH₄ hydrolysis reaction was also calculated from the slope of the Arrhenius plot and found to be E_a = 39.255 kJ.mol⁻¹, as presented in Figure 7c. The reaction appears to be unaffected by changes in temperature due to its relatively low activation energy, and the catalyst's performance at low temperatures is adequate.

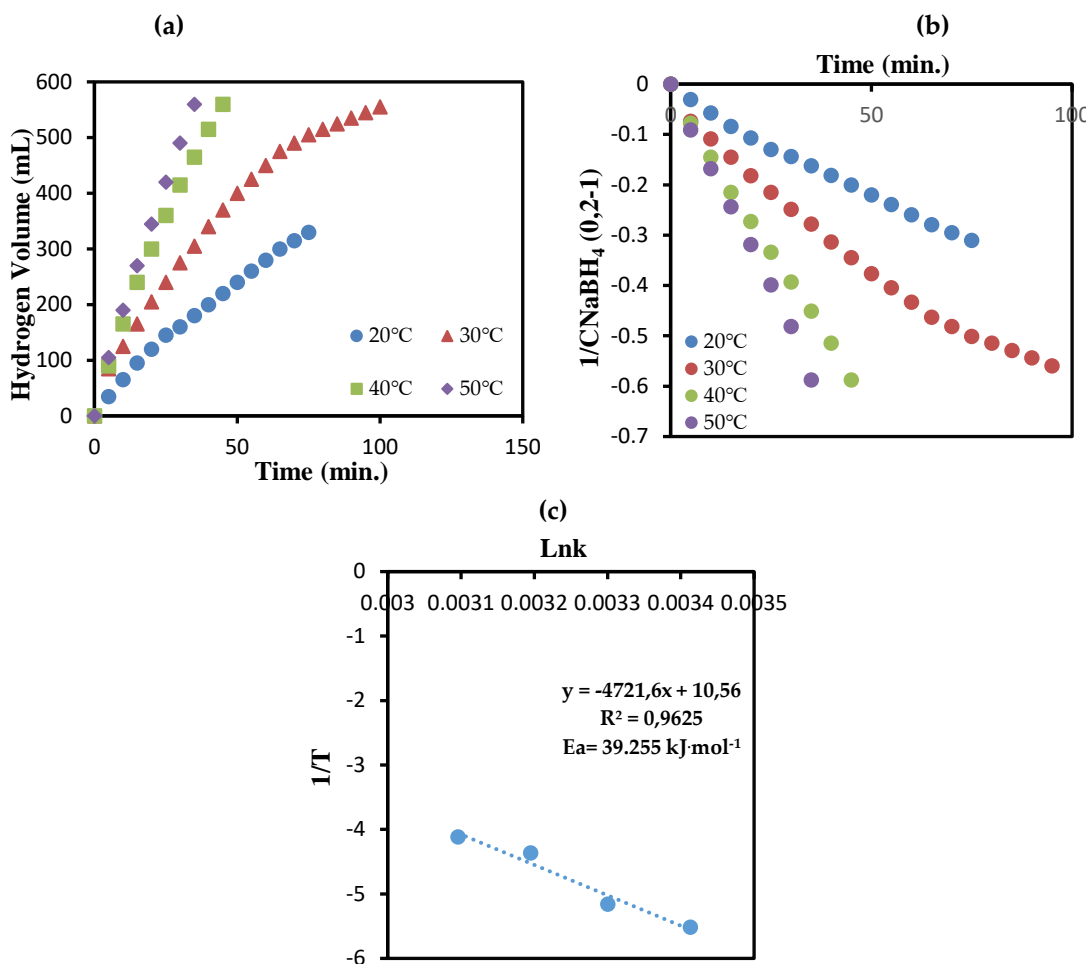


Figure 7. The plot of hydrogen volume versus time with various temperatures with Ni@EC-250 catalyst (a), Linear regression based on n-order at different temperatures (b) and apparent activation energy for Ni@EC-250 catalyst (c)

Table 1 presents a comparison of hydrogen evolution activities between various nickel catalysts. According to the data in Table 1, it is evident that polymer decoration has substantially enhanced the hydrogen evolution rate.

Table 1. The comparison of the hydrogen evolution activities of Nickel catalysts

Catalyst	Hydrogen evolution rate($\text{mL H}_2 \text{g}_{\text{cat}}^{-1} \text{min}^{-1}$)	Activation Energy(kJ mol^{-1})
Ni metal	772	-
Nickel-Imine complex	2240	18.160
Ni@EC	6879	16.633
Ni@EC-250	15576	39.255
Ni@ECM	8830	28.766

3.1.3. Reusability tests of Ni@EC-250 in sodium borohydride hydrolysis reaction

For the catalyst, reusability is essential to determine the catalytic performance. In sodium borohydride hydrolysis, to determine the reusability performance of Ni@EC-250 catalyst, five catalytic cycles were experienced. For this purpose, the reusability tests were performed at 30 °C with 10 % NaOH in 2 % NaBH₄ solution and the results were shown in Figure 8. Before each hydrolysis study, the Ni@EC-250 catalyst was washed and dried several times for the next catalytic cycle in the sodium borohydride hydrolysis reaction. Even if small decreases were observed in the catalytic activity, the reactions resulted with 100 %

conversion in five hydrolysis cycles. These small decreases may have arisen from both by-product filling into the catalyst's pores and the increasing viscosity of the solution. Thus, they caused a decrease in the active sites of the catalyst surface.

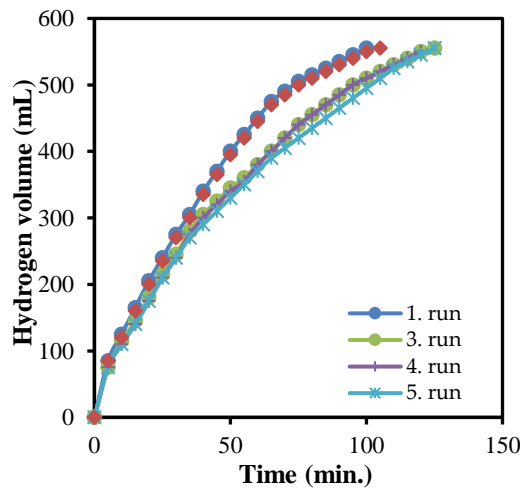


Figure 8. Reusability test results for Ni@EC-250 catalyst in hydrolysis of sodium borohydride reaction

3.2. Characterization

The synthesized polymer-decorated nickel-imine complex catalysts (Ni@EC, Ni@EC-250, and Ni@ECM) characterization occurred using FT-IR, BET, SEM, XRD, XPS, and UV-Vis. Table 2 displays the characteristic infrared spectral values of the nickel complex and the Ni@EC, Ni@EC-250, and Ni@ECM catalysts. The azomethine (-C=N-) group [40], represented by a band at 1621 cm⁻¹ in the nickel-imine complex, shifted to 1628; 1632 and 1629 cm⁻¹ in Ni@EC, Ni@EC-250, and Ni@ECM catalysts, respectively. The changes in observed bands from 2958 cm⁻¹ to 2960; 2964 and 2959 cm⁻¹ for the free -OH vibrations [41] were seen in Ni@EC, Ni@EC-250, and Ni@ECM catalysts, respectively. The Ni@EC, Ni@EC-250, and Ni@ECM catalysts exhibited -C-O vibrations, characterized by shifts in the 1020 cm⁻¹ band to 1047; 1056 and 1051 cm⁻¹ respectively. The FT-IR band related to -CH₃ vibrations remained unaltered in both the nickel-imine complex and the three-polymer-adorned nickel-imine complex catalysts, with a band spotted at 2750-2950 cm⁻¹. The key bands verifying the coordination between metals and ligands (Ni-O and Ni-N) demonstrated certain shifts [42, 43], as displayed in Table 2.

Table 2. Characteristic FT-IR bands of catalysts (cm⁻¹)

Catalyst	$\nu(\text{CH}_3)$	Free $\nu(\text{OH})$	$\nu(\text{C}=\text{N})$	$\nu(\text{C}-\text{O})$	$\nu(\text{M}-\text{O})$	$\nu(\text{M}-\text{N})$
Nickel-Imine complex	2750-2950	2958	1621	1020	495	430
Ni@EC	2750-2950	2960	1628	1047	498	426
Ni@ECM	2750-2950	2964	1632	1056	501	432
Ni@EC-250	2750-2950	2959	1629	1051	496	428

Figure 9 illustrates the electronic spectra of Ni@EC, Ni@EC-250, and Ni@ECM. The three polymer-decorated nickel-imine complexes display comparable electronic behavior. A broad electronic band at 397.55 nm was observed in all three samples, which can be attributed to Ni → Ni charge transfer. Additionally, small bands detected at 316.27 nm were assigned to the n-π* transition of the azomethine group (-C=N-). Furthermore, two different electronic bands were observed, although this was not very apparent. They are located at 324.56 nm (due to the ligand-to-metal charge transfer (LMCT) resulting from the O → Ni charge transfer) and 492.23 nm (due to the d-d transitions (¹A_{1g} → ¹A_{2g}) of the Ni ion), respective.

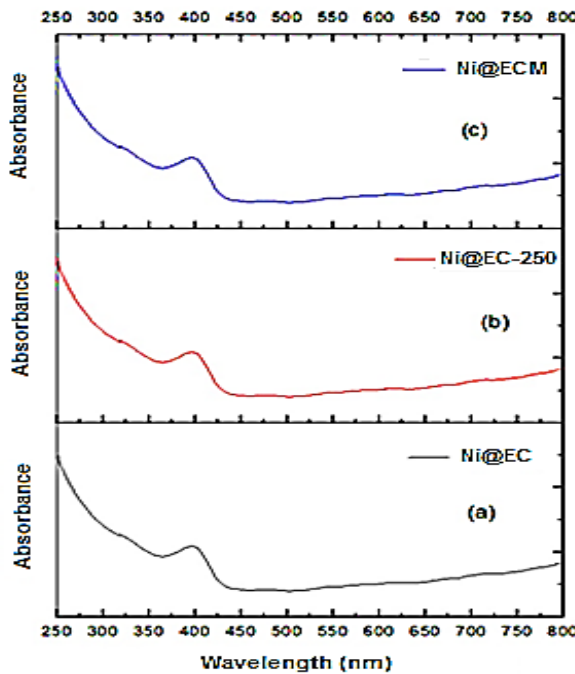


Figure 9. The UV-Vis spectrum of Ni@EC, Ni@EC-250, Ni@ECM

Fig.10a displays the XRD patterns for Ni@EC, Ni@EC-250 and Ni@ECM. The patterns reveal that the crystalline phase was present in the synthesized polymer-decorated nickel-imine complex catalysts. The polymer-decorated nickel complex catalysts exhibit sharp crystalline XRD patterns, which are caused by the natural crystalline properties of the nickel complex. The size of the crystallites for Ni@EC, Ni@EC-250, and Ni@ECM were assessed using Scherre's formula, by measuring the full width at half maximum of the corresponding XRD peaks. The obtained data indicates that the synthesized nickel-imine complexes decorated with polymer are monocrystalline. Specifically, the crystallite sizes of the Ni@EC, Ni@EC-250 and Ni@ECM samples are 29°, 38°, and 59° respectively.

X-ray photoelectron spectroscopy (XPS) was used to determine the electronic properties of the species on the catalyst surface. A clear presence of Ni@EC, Ni@EC-250 and Ni@ECM, which confirm the respective oxidation states of the elements, is shown in Figure 10b. The XPS traces of Ni@EC, Ni@EC-250 and Ni@ECM were determined to be around 885 eV for Ni (II) (2p), which confirms the diamagnetic structure of the nickel-imine complex. X-ray photoelectron spectroscopy traces of Ni@EC, Ni@EC-250, and Ni@ECM demonstrated binding energy values of 862.1 eV and 879.9 eV for the 2p^{3/2} and 2p^{1/2} conditions, respectively.

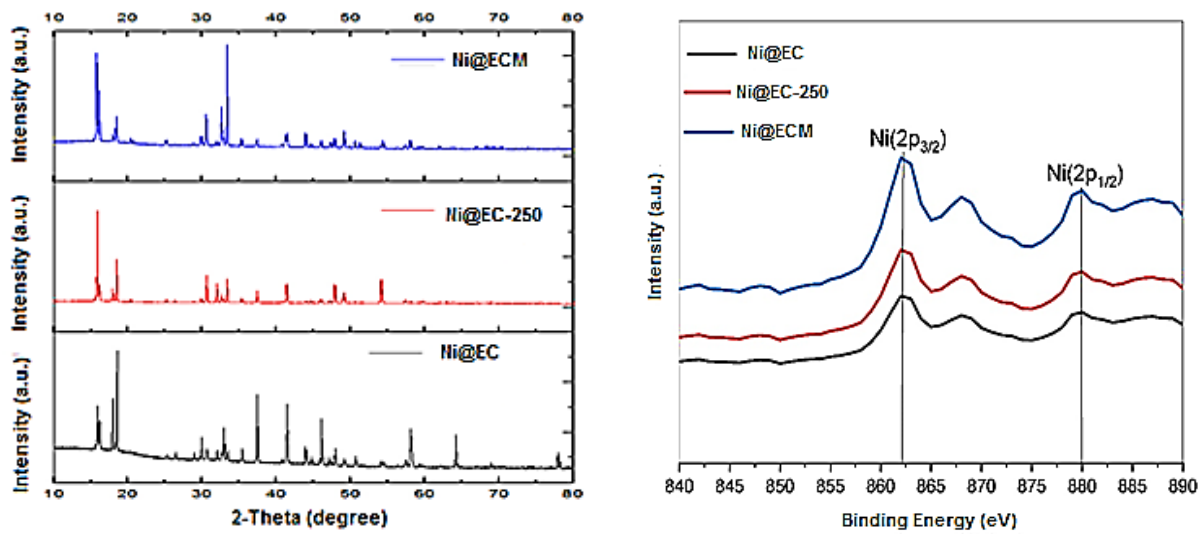


Figure 10. The XRD patterns Ni@EC, Ni@EC-250, and Ni@ECM (a) and XPS traces of Ni@EC, Ni@EC-250 and Ni@ECM (b)

Figure 11a shows the recorded SEM image of the Ni@EC sample. As can be seen from the figure, there is an agglomerated spherical image. It is seen that the Nickel-Imine complex was well distributed on polymers. Based on the size scale given in the SEM image, the average crystallite size of the Ni@EC sample is less than 100 nm. It shows a similar image in the Ni@EC-250 example given in Figure 11b. Unlike the Ni@EC sample, the particles are separated from each other in the Ni@EC-250 sample. Rather than a spherical structure, a bar image is observed. The SEM image shown in Figure 11c is from the Ni@ECM sample. The sample synthesized in the figure has been observed to be in the form of nanoscale wire. When examined dimensionally, the crystallite size of the Ni@ECM sample was less than 100 nm. Thus, it was realized that the crystallite size obtained for all three samples coincided with the crystallite size data obtained from XRD measurements.

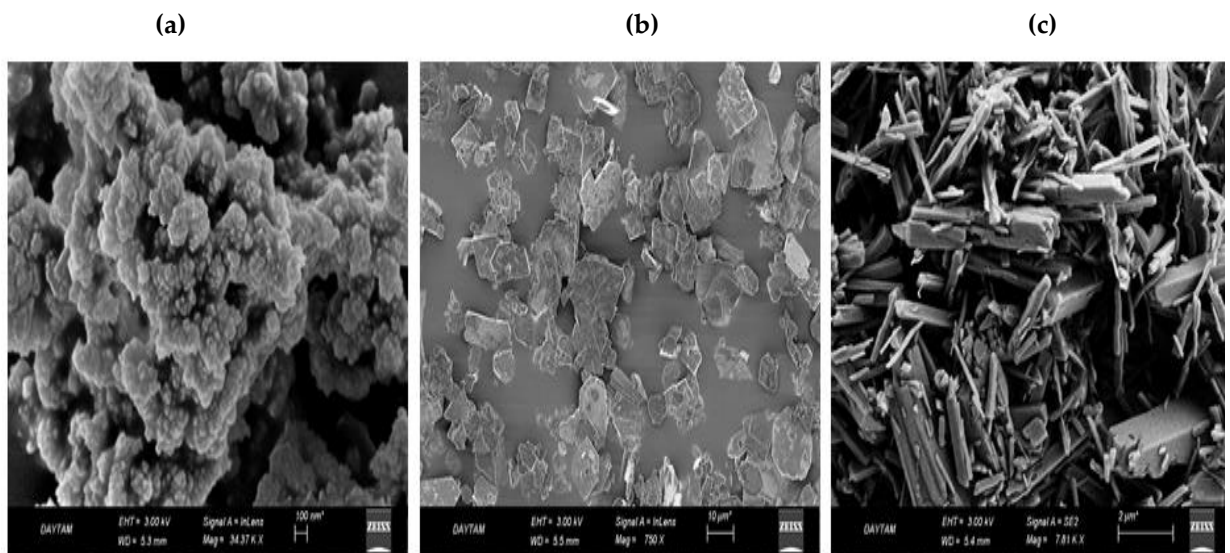


Figure 11. The SEM images of Ni@EC (a), Ni@EC-250 (b) and Ni@ECM (c)

The specific surface areas, total pore volumes, and average pore sizes of the nickel-imine complex, Ni@EC, Ni@EC-250, and Ni@ECM catalysts are presented in Table 3. The polymer-decorated nickel-imine complex catalysts had surface areas of 58.721; 56.365 and 52.849 m²/g for Ni@EC, Ni@EC-250 and Ni@ECM catalysts, respectively. Technical term abbreviations were explained upon the first usage. In contrast, the

surface area of the nickel complex was measured to be $48.456 \text{ m}^2/\text{g}$. It can be observed that the Ni@EC, Ni@EC-250, and Ni@ECM catalysts exhibit larger surface areas compared to the nickel-imine complex. The pore volume of the nickel-imine complex was found to be smaller at $0.178 \text{ cm}^3\cdot\text{g}^{-1}$ as opposed to the Ni@EC, Ni@EC-250 and Ni@ECM catalysts which had pore volumes of 0.253 ; 0.211 and $0.230 \text{ cm}^3\cdot\text{g}^{-1}$ respectively. These outcomes suggest that the larger surface area of the catalysts is attributed to the presence of larger active sites leading to enhanced hydrogen evolution performance.

Table 3. BET analysis results of catalysts

Catalyst	$S_{\text{BET}} (\text{m}^2 \cdot \text{g}^{-1})$	Average pore	Pore volume
Nickel-Imine complex	48.456	14.743	0.178
Ni@EC	58.210	21.194	0.253
Ni@EC-250	56.365	18.296	0.211
Ni@ECM	52.849	17.885	0.230

4. CONCLUSIONS

In this study, the initial objective was to synthesize three new and effective catalysts for the hydrolysis of sodium borohydride to produce hydrogen. To achieve this, a Nickel-Imine complex was combined with three distinct polymers (EC, EC-250, and ECM) to enlarge the surface area of Nickel-Imine and enhance the catalytic interaction with sodium borohydride. According to the experimental results, the catalysts obtained, i.e., Ni@EC, Ni@EC-250, and Ni@ECM, exhibited exceptional performance in hydrolysis of sodium borohydride with hydrogen evolution rates of 6879 ; 15576 ; $8830 \text{ mL H}_2 \text{ gcat}^{-1}\cdot\text{min}^{-1}$ and 15459 ; $28,689$; $23,417 \text{ mL H}_2 \text{ gcat}^{-1}\cdot\text{min}^{-1}$ at 30°C and 50°C , respectively. It is evident that the polymer decoration remarkably enhances the hydrogen evolution rate. Whereas the pure Nickel-Imine complex showed lower activity, with $2240 \text{ mL H}_2 \text{ gcat}^{-1}\cdot\text{min}^{-1}$, compared to Ni metal which was only $772 \text{ mL H}_2 \text{ gcat}^{-1}\cdot\text{min}^{-1}$ at the same temperatures, the decoration of the Ni-Imine complex with polymers on its surface area increased the catalyst's surface area, resulting in improved hydrogen evolution rates. The activation energies of the Ni@EC, Ni@EC-250, and Ni@ECM catalysts were calculated to be $16.633 \text{ kJ}\cdot\text{mol}^{-1}$, $39.255 \text{ kJ}\cdot\text{mol}^{-1}$, and $28.766 \text{ kJ}\cdot\text{mol}^{-1}$, respectively. In the second step, the objective was to determine the catalyst with the best catalytic performance among the three options. Out of all the decorated catalysts, Ni@EC-250 catalyst showed the best activity under the same conditions compared to Ni@EC and Ni@ECM. With the addition of the polymer, the catalytic activity increased in the order of $\text{Ni@EC-250} > \text{Ni@ECM} > \text{Ni@EC}$. As a result, Ni@EC-250 was selected for the remaining steps of the catalytic hydrolysis reaction. The results of the reusability tests indicate that Ni@EC-250 remains active in sodium borohydride hydrolysis even after the fifth run, achieving 100 % conversions.

Declaration of Ethical Standards

The authors declare that all ethical guidelines including authorship, citation, data reporting, and publishing original research are followed.

Credit Authorship Contribution Statement

Dilek KILINÇ: Investigation, Experimental Section, Data curation, Methodology, Original draft preparation, Writing- Reviewing-Editing, Validation. **Ömer ŞAHİN:** Methodology, Validation

Declaration of Competing Interest

The authors declare that they have no known competing financial interests or personal relationships that could have appeared to influence the work reported in this paper.

Funding / Acknowledgements

This work was supported by the Research Centre of Siirt University (Project number 2017-SIUFED-67).

REFERENCES

- [1] D. Kilinç, O. Sahin, C. Saka, "Investigation on salicylaldimine-Ni complex catalyst as an alternative to increasing the performance of catalytic hydrolysis of sodium borohydride," *International Journal of Hydrogen Energy*, vol. 42, pp. 20625-20637, 2017.
- [2] S. Santra, D. Das, N.S. Das, K.K. Nanda, "An efficient on-board metal-free nanocatalyst for controlled room temperature hydrogen production," *Chemical Science*, vol. 8, pp.2994-3001, 2017.
- [3] L. Semiz, N. Abdullayeva, M. Sankir, "Nanoporous Pt and Ru catalysts by chemical dealloying of Pt-Al and Ru-Al alloys for ultrafast hydrogen generation," *Journal of Alloys Compounds*, vol. 744, pp. 110-115, 2018.
- [4] M.Z. Jacobson, W.G. Colella, D.M. Golden, "Cleaning the air and improving health with hydrogen fuel-cell vehicles," *Science*, vol. 308, pp. 1901-1905, 2005.
- [5] D. Huang, P. Zhao, F. Fu, J. Wie, X. Yang, D. Astruc, C. Wang, J. Zhu, C. Luo, "Highly efficient and selective Co@ZIF-8 nanocatalyst for hydrogen release from sodium borohydride hydrolysis, *ChemCatChem*," vol. 11, pp. 1643-1649, 2019.
- [6] M. Sankir, L. Semiz, R.B. Serin, N.D. Sankir, "Hydrogen generation from nanoflower platinum films," *International Journal of Hydrogen Energy*, vol. 40, pp. 8522–8529, 2015.
- [7] S.C. Li, F.C. Wang, "The development of a sodium borohydride hydrogen generation system for proton exchange membrane fuel cell," *International Journal of Hydrogen Energy*, vol. 41, pp. 3038–3051, 2016.
- [8] M. Sankir, R.B. Serin, L. Semiz, N.D. Sankir, "Unusual behavior of dynamic hydrogen generation from sodium borohydride," *International Journal of Hydrogen Energy*, vol. 39, pp. 2608–2613, 2014.
- [9] F. Ali, S.B. Khan, A.M. Asiri, "Chitosan coated cellulose cotton fibers as catalyst for the H₂ production from NaBH₄ methanolysis," *International Journal of Hydrogen Energy*, vol. 44, pp. 4143–4155, 2014.
- [10] C. Huff, T. Dushatinski, T.M. Abdel-Fattah, "Gold nanoparticle/multi-walled carbon nanotube composite as novel catalyst for hydrogen evolution reactions," *International Journal of Hydrogen Energy*, vol. 42, pp. 18985–18990, 2017.
- [11] D. Kilinç, "Effect of Al₂O₃-supported Cu-Schiff base complex as a catalyst for hydrogen generation in NaBH₄ hydrolysis," *Energy Sources Part A-Recovery Utilization and Environmental Effects*, vol. 40, pp. 873-885, 2018.
- [12] E. Fangaj, A.A. Ceyhan, "Apricot Kernel shell waste treated with phosphoric acid used as a green, metal-free catalyst for hydrogen generation from hydrolysis of sodium borohydride," *International Journal of Hydrogen Energy*, vol. 45, pp. 17104-17117, 2020.
- [13] D. Kilinc, O. Sahin, "Effective TiO₂ supported Cu-Complex catalyst in NaBH₄ hydrolysis reaction to hydrogen generation," *International Journal of Hydrogen Energy*, vol. 44: pp. 18858-18865, 2019.
- [14] O. Akdim, U.B. Demirci, D. Muller, P. Miele, "Cobalt (II) salts, performing materials for generating hydrogen from sodium borohydride," *International Journal of Hydrogen Energy*, vol. 34, pp. 2631-7, 2019.
- [15] J. Andrieux, D. Swierczynski, L. Laversenne, A. Garron, S. Bennici, C. Goutaudier, et al., "Amultifactor study of catalyzed hydrolysis of solid NaBH₄ on cobalt nanoparticles: thermodynamics and kinetics," *International Journal of Hydrogen Energy*, vol. 34, pp. 938-51, 2019.
- [16] O. Akdim, U.B. Demirci, P. Miele, "Acetic acid, a relatively green single-use catalyst for hydrogen

- generation from sodium borohydride," International Journal of Hydrogen Energy, vol. 34, pp. 7231-8, 2009.
- [17] Y. Kojima, K.I. Suzuki, K. Fukumoto, M. Sasaki, T. Yamamoto, Y. Kawai, et al., "Hydrogen generation using sodium borohydride solution and metal catalyst coated on metal oxide," International Journal of Hydrogen Energy, vol. 27, pp. 1029-34, 2002.
- [18] D. Xu, X. Lai, W. Guo, X. Zhang, C. Wang, P. Dai, "Efficient catalytic properties of SO₄²⁻ / M_xO_y (M = Cu, Co, Fe) catalysts for hydrogen generation by methanolysis of sodium borohydride," International Journal of Hydrogen Energy, vol. 43, pp. 6594-6602, 2018.
- [19] X. Zhang, X. Sun, D. Xu, X. Tao, P. Dai, Q. Guo, X. Liu, " Synthesis of MOF-derived Co@C composites and application for efficient hydrolysis of sodium borohydride, Applied Surface Science, vol. 469, pp. 764-769, 2019.
- [20] D. Kilinc, Ö. Sahin, "Ruthenium-Imine Catalyzed KBH₄ Hydrolysis as an Efficient Hydrogen Production System, International Journal of Hydrogen Energy, vol. 46, pp. 20984-20994, 2021.
- [21] D. Kilinc, O. Sahin "Highly active and stable CeO₂ supported nickel complex catalyst in hydrogen generation," International Journal of Hydrogen Energy, vol. 46, pp. 499-507, 2022.
- [22] J. Lee, H. Shin, K.S. Choi, J. Lee, J.Y. Choi, H.K. Yu, "Carbon layer supported nickel catalyst for sodium borohydride (NaBH₄) dehydrogenation," International Journal of Hydrogen Energy, vol. 44 pp. 2943-2950, 2019.
- [23] A.A. Ceyhan, S. Edebalı, E. Fangaj, "A study on hydrogen generation from NaBH₄ solution using Co-loaded resin catalysts," International Journal of Hydrogen Energy, vol. 45, pp. 45:34761-34772, 2020.
- [24] A. Pozio, M. De Francesco, G. Monteleone, R. Oronzio, S. Galli, C. D'Angelo, et al., "Apparatus for the production of hydrogen from sodium borohydride in alkaline solution," International Journal of Hydrogen Energy, vol. 33, pp. 51-56, 2008.
- [25] N. Patel, R. Fernandes, N. Bazzanella, A. Miotello, "Co-P-B catalyst thin films prepared by electroless and pulsed laser deposition for hydrogen generation by hydrolysis of alkaline sodium borohydride: a comparison," Thin Solid Films, vol. 518, pp. 4779-4785, 2010.
- [26] S.C. Amendola, S.L. Sharp-Goldman, M. Saleem Janjua, N.C. Spencer, M.T. Kelly, P.J. Petillo, et al., "A safe, portable, hydrogen gas generator using aqueous borohydride solution and Ru catalyst," International Journal of Hydrogen Energy vol. 25, pp. 969-75, 2010.
- [27] J.P. Holgado, J. Morales, A. Caballero, A.R. Gonza'lez-Elipe, "Plate reactor for testing catalysts in the form of thin films," Applied Catalysis B: Environment and Energy, vol. 31, pp. 31-36, 2001.
- [28] N. Malvadkar, S. Park, "Urquidi-MacDonald M, Wang H, Demirel MC. Catalytic activity of cobalt deposited on nanostructured poly(p-xyllylene) films," Journal of Power Source, vol. 182, pp. 323-8, 2008.
- [29] D. Kilinc, "Co complex modified on Eupergit C as a highly active catalyst for enhanced hydrogen production," International Journal of Hydrogen Energy, vol. 47, pp. 11894-11903, 2022.
- [30] D. Kilinc, O. Sahin, C. Saka, "Salicylaldimine-Ni complex supported on Al₂O₃: Highly efficient catalyst for hydrogen production from hydrolysis of sodium borohydride," International Journal of Hydrogen Energy, vol. 43, pp. 251-261, 2018.
- [31] D. Kilinc, Ö. Sahin, "Synthesis of polymer supported Ni (II)-Schiff Base complex and its usage as a catalyst in sodium borohydride hydrolysis," International Journal of Hydrogen Energy, vol. 43, pp. 10717-10727, 2018.
- [32] G.P. Rachiero, U.B. Demirci, P. Miele, "Bimetallic RuCo and RuCu catalysts supported on γ-Al₂O₃. A comparative study of their activity in hydrolysis of ammonia-borane," International Journal of Hydrogen Energy, vol. 36, pp. 7051-7065, 2011.
- [33] J.Q. Wu, D.L. Wang, X.M. Xu, N.B. Long, R.F. Zhang, "Efficient synthesis of DHA/EPA-rich phosphatidylcholine by inhibition of hydrolysis reaction using immobilized phospholipase A1 on macroporous SiO₂/cationic polymer nano-composited support," Molecular Catalysis, vol. 499, pp. 111278, 2021.

- [34] M. Grigoras, C.O. Catanesu, "Imine oligomers and polymer," *Journal of Macromolecular Science, Part C: Polymer Reviews*, vol. 44, pp. 131-173, 2004.
- [35] D. Kılınç, O. Sahin, S. Horoz, "Use of low-cost Zn (II) complex efficiently in a dye-sensitized solar cell device," *Journal of Materials Science: Materials in Electronics*, vol. 30, pp. 11464-11467, 2019.
- [36] A. Xavier, N. Srividhya, "Synthesis and study of Schiff base ligands," *Journal of Applied Chemistry*, vol. 7, pp. 6-15, 2014.
- [37] M.S. Karthikeyan, D.J. Prasad, B. Poojary, K.S. Bhat, B.S. Holla, N.S. Kumari, "Synthesis and biological activity of Schiff and Mannich bases bearing 2, 4-dichloro-5-fluorophenyl moiety," *Bioorganic & Medicinal Chemistry*, vol.14, pp. 7482-7489, 2006.
- [38] D. Kılınç, O. Sahin "High volume hydrogen evolution from KBH₄ hydrolysis with palladium complex catalyst," *Renewable Energy*, vol. 161, pp. 257-264, 2019.
- [39] D. Kılınç, O. Sahin "Development of highly efficient and reusable Ruthenium complex catalyst for hydrogen evolution," *International Journal of Hydrogen Energy*, vol. 47, pp. 3876-3885, 2022.
- [40] K. Nejati, Z. Rezvani, "Syntheses, characterization and mesomorphic properties of new bis(alkoxyphenylazo)- substituted N, N' salicylidene diiminato Ni (II), Cu (II) and VO(IV) complexes," *New J Chem*, vol. 27, pp. 1665, 2003.
- [41] K. Naresh Kumar K, R. Ramesh, "Synthesis, luminescent, redox and catalytic properties of Ru (II) carbonyl complexes containing 2N₂O donors," *Polyhedron*, vol. 24, pp. 1885-92, 2005.
- [42] T. Rosu, E. Pahontu, C. Maxim, R. Georgescu, N. Stanica, A. Gulea, "Some new Cu (II) complexes containing an on-donor Schiff base: synthesis, characterization and antibacterial activity," *Polyhedron*, vol. 30, pp. 154-62, 2011.
- [43] M.R.P. Kurup, B. Varghese, M. Sithambaresan, S. Krishnan, S.R. Sheeja, E. Suresh, "Synthesis, spectral characterization and crystal structure of copper (II) complexes of 2- benzoyl pyridine-N (4)-phenyl semicarbazone," *Polyhedron*, vol.30, pp. 70-8, 2011.